Peer-reviewed version available at *Int. J. Mol. Sci.* **2020**, *21*, 1154; doi:10.3390/ijms21031154

# Chronic Mild Stress Modified Epigenetic Mechanisms Leading to Accelerated Senescence and Impaired Cognitive Performance in Mice

Puigoriol-Illamola, D[1,3]; Martínez-Damas, M[2]; Griñán-Ferré, C[1,3*] and Pallàs, M[1,3*].

[1]Pharmacology Section, Department of Pharmacology, Toxicology and Therapeutic Chemistry. Faculty of Pharmacy and Food Sciences. University of Barcelona, Av Joan XXIII 27-31, 08028 Barcelona, Spain.

[2]Institute of Biomedical Research (IIBO), Universidad Nacional Autónoma de México (UNAM). Subdirección de Enseñanza e Investigación, División de Investigación Biomédica, Centro Médico Nacional 20 de Noviembre. México City, México.

[3]Institute of Neuroscience, University of Barcelona (NeuroUB), Barcelona, Spain.

*These authors contributed equally

Corresponding author:
Mercè Pallàs, PhD.

Pharmacology Section in Pharmacology, Toxicology, and Therapeutic Chemistry Department, Faculty of Pharmacy and Food Sciences, University of Barcelona, Av Joan XXIII 27-31, 08028 Barcelona, Spain.
e-mail: pallas@ub.edu

**Keywords:** Stress; epigenetics; senescence; cognition; age-related cognitive decline; Alzheimer's disease; SAMP8; SAMR1; oxidative stress; inflammation; autophagy.

**Abstract**

Cognitive and behavioural disturbances are growing public healthcare issue for the modern society, as stressful lifestyle is becoming more and more common. Besides, several pieces of evidence state that environment is crucial in the development of several diseases as well as compromising healthy aging. Therefore, it is important to study the effects of stress on cognition and its relationship with aging.

To address these queries, Chronic Mild Stress (CMS) paradigm was used in the senescence-accelerated mouse prone 8 (SAMP8) and resistant 1 (SAMR1). On one hand, we determined the changes produced in the three main epigenetic marks after 4 weeks of CMS treatment, such as a reduction in histone posttranslational modifications and DNA methylation, and up-regulation or down-regulation of several miRNA involved in different cellular processes in mice. In addition, CMS treatment induced reactive oxygen species (ROS) accumulation and loss of antioxidant defence mechanisms, as well as inflammatory signalling activation through NF-κB pathway and astrogliosis markers, like Gfap. Remarkably, CMS altered mTORC1 signalling in both strains, decreasing autophagy only in SAMR1 mice.

We found a decrease in glycogen synthase kinase 3 β (GSK-3β) inactivation, hyperphosphorylation of Tau and an increase in sAPPβ protein levels in mice under CMS. Moreover, reduction in the non-amyloidogenic secretase ADAM10 protein levels was found in SAMR1 CMS group. Consequently, detrimental effects on behaviour and cognitive performance were detected in CMS treated mice, affecting mainly SAMR1 mice, promoting a turning to SAMP8 phenotype. In conclusion, CMS is a feasible intervention to understand the influence of stress on epigenetic mechanisms underlying cognition and accelerating senescence.

## 1. Introduction

Aging is a multifactorial process characterized by a progressive loss of physiological integrity, resulting in an impaired function and increased vulnerability to death. Physiological brain aging involves cognitive loss, which includes decreased learning and memory abilities and slower responses to different stimulus [1]. Indeed, normal aging differs from pathological aging and this might be explained by the lifestyle. Environmental factors drive epigenetic modifications resulting in phenotypic differences, which alter almost all tissues and organs. Although the brain is one of the most affected structures, such modifications lead to a progressive decline in the cognitive function and create a favourable context for the development of neurodegenerative diseases [2]. Aging is the most significant risk factor for most chronic diseases, such as age-related cognitive decline and Alzheimer's disease (AD) [3]. In fact, AD is the most prevalent dementia and its progression is influenced by both genetic and environmental factors [4].

Several studies define that a good environment is essential to enhance learning and cognitive abilities, besides the continued presence of stressors is associated with the opposite effects. Epigenetics refers to potentially heritable and environmentally modifiable changes in gene expression mediated via non-DNA encoded mechanisms [5]. Recent evidence has demonstrated significant associations between epigenetic alterations and stress [2,6]. Potential threats cause a course of action releasing numerous transmitters and hormones throughout our body, particularly catecholamines and glucocorticoids. The interaction of glucocorticoids and adrenergic systems in specific brain regions has proved an essential mediating mechanism for a wide variety of actions displayed by stress on cognition [7]. Firstly, stress response allows body adaptation. However, when stress is prolonged it has been shown that decreases synaptic plasticity [8], alters hippocampal volume [9,10] and neurotransmitters [11] and may lead to Alzheimer's disease [12]. Concretely, chronic stress is associated with increased Aβ deposits and hyperphosphorylated Tau [13].

Oxidative stress (OS) and inflammation are deeply involved in age-related deleterious disorders. Along with the aging process, several factors, such as a naturally decreased

capacity of the antioxidant enzymes system, create an imbalance between antioxidant mechanisms and reactive oxygen system (ROS)-production equilibrium, accumulating ROS beyond the detoxifying capacity of the antioxidant system resulting in OS, eventually causing cellular damage that can no longer be repaired by internal mechanisms, finally causing the dysfunction of the system [14]. In addition, one of the major changes while aging is the dysregulation of the immune response, leading to chronic systemic inflammatory state [15]. Overall, OS misbalance, mitochondrial dysfunction and the inflammatory response have been linked to accelerate aging and fasten progression of neurodegenerative diseases [14,16]. Moreover, accumulation of dysfunctional and damaged cellular proteins and organelles occurs during aging, resulting in a disruption of cellular homeostasis and progressive degeneration and increasing the risk of cell death [17]. Autophagy is particularly important in the maintenance of homeostasis, as it participates in the elimination of disrupted proteins and molecules and helps to maintain a clean cellular environment. It has been widely described that there are alterations in autophagy while aging as well as in age-related cognitive decline, AD and other dementias [18-20]. Moderating all these detrimental components is key in the promotion of cell survival and longevity.

The senescence-accelerated mouse (SAM) models include senescence-accelerate prone (SAMP) and senescence-accelerated resistant (SAMR) mice [21]. SAMP8 strain has been widely used as an aging model for the study of brain aging and age-related pathologies. Its cognitive impairment is associated with alterations in both hippocampal structure and activity, causing oxidative stress misbalance and driving to AD neuropathology, such as tau- and amyloid-related alterations [1,22]. On the contrary, SAMR1 strain manifests a normal aging process.

Understanding the epigenetic modifications that stressful environment triggers in neurodegeneration mechanisms is essential to develop novel therapeutics for age-related cognitive decline. This study aims to determine the effects on brain function of a stressful lifestyle in an animal model with accelerated senescence, SAMP8, and in the resistant senescence strain, SAMR1.

## 2. Materials and methods

### 2.1. Animals and Chronic Mild Stress Procedure

Females SAMP8 mice (n=56) were used to carry out behavioural, cognitive and molecular analyses. We divided these animals into four groups: SAMR1 (SAMR1 Control, n=14), SAMR1 treated with CMS (SAMR1 CMS, n=14), SAMP8 (SAMP8 Control, n=14) and SAMP8 treated with CMS (SAMP8 CMS, n=14). Animals had free access to food and water and were kept under standard temperature conditions (22±2°C) and 12h: 12h light-dark cycles (300lux/0 lux). Starting at 4 months of age, CMS groups received the Chronic Mild Stress (CMS) treatment. CMS procedure that was used in the present study had previously been validated in SAMR1 and SAMP8 mice, with some modifications [22]. Mice were exposed to various randomly scheduled, low-intensity environmental stressors every day for 4 weeks. Different stressful stimuli were applied every day and the sequence of the stressors was altered every week to guarantee the degree of unpredictability. Among others, CMS stimulus were 24h of water deprivation, 24h of food deprivation, 2h of physical restraint, 24h of sawdust removal, 24h of wet bedding, overnight illumination and 1min of tail nipping at 1cm from the tip of the tail. Before the performance of the cognitive tests, the glucose tolerance test was conducted.

All experimental procedures involving animals were performed followed by standard ethical guidelines European Communities Council Directive 86/609/EEC and by the Institutional Animal Care and Use Committee of the University of Barcelona (670/14/8102, approved at 11/14/2014) and by Generalitat de Catalunya (10291, approved 1/28/2018). All efforts were made to minimize the number of mice used and their suffering.

### 2.2. Glucose tolerance test

Intraperitoneal (i.p.) glucose tolerance test was performed following 4 weeks of CMS treatment, as described previously. In brief, mice fasted overnight for 12h. The test was performed in a quiet room and 2g/kg i.p. glucose injection was administered (diluted in $H_2O$) and blood glucose levels were measured at 0, 5, 10, 15, 30, 60 and 120

min after the injection with the Accu-Chek® Aviva blood glucose meter (Accu-Chek® Aviva, Roche, Barcelona, Spain).

### 2.3. Behavioural and cognitive test

#### 2.3.1. Open Field Test (OFT)

The OFT was performed as previously described in Griñán-Ferré et al. [23]. Mice were placed at the centre of a white polywood box (50x50x25cm) and allowed to explore it for 5 minutes. Behaviour was scored with SMART® ver.3.0 software and each trial was recorded for later analysis. The parameters scored included centre staying duration, rearing, grooming and the distance travelled.

#### 2.3.2. Novel Object Recognition Test (NORT)

The Novel Object Recognition Test (NORT) protocol employed was as described in Puigoriol-Illamola et al. [24]. In brief, mice were placed in a 90°, two-arms, 25cm-long, 20cm-high, 5cm-wide black maze. Before performing the test, the mice were individually habituated to the apparatus for 10min for 3 days. On day 4, the animals were submitted to a 10min acquisition trial (first trial), during which they were placed in the maze in the presence of two identical, novel objects at the end of each arm. After a delay (2h and 24h), the animal was exposed to two objects one old object and one novel object. The Time that mice explored the Novel object (TN) and Time that mice explored the Old object (TO) were measured. A Discrimination Index (DI) was defined as (TN−TO)/(TN+TO). To avoid object preference biases, objects were counterbalanced. The maze, the surface, and the objects were cleaned with 70% ethanol between the animals' trials to eliminate olfactory cues.

#### 2.3.3. Morris Water Maze (MWM)

This test evaluates both learning and spatial memory [25]. An open circular pool (100 cm in diameter, 50 cm in height) filled with water was used. Water was painted white with latex in order to make it opaque and its temperature was 22± 1°C. Two main perpendicular axes were established (North-South and East-West), thus configuring four equal quadrants (NE, NW, SE, and SW). Four visual clues (N, S, E, W) were placed on the walls of the tank so that the animal could orientate and could fulfil the objective. The test consists of training a mouse to find a submerged platform (Learning

phase) and assess whether the animal has learned and remembered where the platform was the day that it is removed (Test). The training lasts five consecutive days and every day five trials are performed, which have a different starting point (NE, E, SE, S, and SW), with the aim that the animal recognizes the visual clues and learns how to locate the platform, avoiding learning the same path. At each trial, the mouse was placed gently into the water, facing the wall of the pool, allowed to swim for 60 seconds and there was not a resting time between trials. If the animal was not able to locate the platform, the investigator guided it to the platform and was allowed to rest and orientate for 30 seconds. The platform was placed approximately in the middle of one of the quadrants, 1.5 cm below the water level. Above the pool there was a camera that recorded the animals' swimming paths and the data was analysed with the statistical program SMART® ver.3.0. During the learning phase, a learning curve was drawn, in which is represented the latency to find the platform every training day. On the day test, more parameters were measured, such as the target crossings and the swum distance in the platform zone.

### 2.4. Immunodetection experiments

#### 2.4.1. Brain processing

Three days after the behavioural and cognitive tests, animals were euthanized for protein extraction, RNA and DNA isolation. Brains were immediately removed, and the hippocampus was isolated, frozen on powdered dry ice and maintained at -80°C until procedures.

#### 2.4.2. Western blotting

Tissue samples were homogenized in lysis buffer (Tris HCl pH 7.4 50mM, NaCl 150mM, EDTA 5mM and 1X-Triton X-100) containing phosphatase and protease inhibitors (Cocktail II, Sigma-Aldrich) to obtain total protein homogenates. Aliquots of 15 µg of hippocampal protein extraction per sample were used. Protein samples were separated by Sodium dodecyl sulphate-polyacrylamide gel electrophoresis (SDS-PAGE) (8-14%) and transferred onto Polyvinylidene difluoride (PVDF) membranes (Millipore). Afterwards, membranes were blocked in 5% non-fat milk in Tris-buffered saline (TBS) solution containing 0.1% Tween 20 TBS (TBS-T) for 1 hour at room temperature, followed by overnight incubation at a 4°C with the primary antibodies listed in

(Supplementary Table 1). Then, the membranes were washed and incubated with secondary antibodies listed in (Supplementary Table 1) for 1 hour at room temperature. Immunoreactive proteins were viewed with the chemiluminescence-based ChemiLucent™ detection kit, following the manufacturer's protocol (ECL Kit, Millipore), and digital images were acquired using ChemiDoc XRS+System (BioRad). Semi-quantitative analyses were done using ImageLab software (BioRad) and results were expressed in Arbitrary Units (AU), considering control protein levels as 100%. Protein loading was routinely monitored by immunodetection of Glyceraldehyde-3-phosphate dehydrogenase (GAPDH) or β-tubulin.

**2.5. RNA extraction and gene expression determination by q-PCR**

Total RNA isolation was carried out using TRIsure™ reagent according to the manufacturer's instructions (Bioline Reagent, UK). The yield, purity, and quality of RNA were determined spectrophotometrically with a NanoDrop™ ND-1000 (Thermo Scientific) apparatus and an Agilent 2100B Bioanalyzer (Agilent Technologies). RNAs with 260/280 ratios and RIN higher than 1.9 and 7.5, respectively, were selected. Reverse Transcription-Polymerase Chain Reaction (RT-PCR) was performed as follows: 2 µg of messenger RNA (mRNA) was reverse-transcribed using the High Capacity cDNA Reverse Transcription Kit (Applied Biosystems). Real-time quantitative PCR (qPCR) was used to quantify mRNA expression of oxidative stress and inflammatory genes listed in (Supplementary Table 2). SYBR® Green real-time PCR was performed in a Step One Plus Detection System (Applied-Biosystems) employing SYBR® Green PCR Master Mix (Applied-Biosystems). Each reaction mixture contained 6.75 µL of complementary DNA (cDNA) (which concentration was 2 µg), 0.75 µL of each primer (which concentration was 100 nM), and 6.75 µL of SYBR® Green PCR Master Mix (2X).

Data were analysed utilizing the comparative Cycle threshold (Ct) method (ΔΔCt), where the housekeeping gene level was used to normalize differences in sample loading and preparation [31]. Normalization of expression levels was performed with β-actin for SYBR® Green-based real-time PCR results. Each sample was analysed in duplicate, and the results represent the n-fold difference of the transcript levels among different groups.

### 2.6. Global DNA Methylation and Hydroxymethylation Determination

Isolation of genomic DNA was conducted using the FitAmp™ Blood and Cultured Cell DNA Extraction Kit (EpiGentek, Farmingdale, NY, USA) according to the manufacturer's instructions. Following this, Methylflash Methylated DNA Quantification Kit (Epigentek, Farmingdale, NY, USA) and MethylFlash HydroxyMethylated DNA Quantification Kit were used in order to detect methylated and hydroxymethylated DNA. Briefly, these kits are based on specific antibody detection of 5-mC and 5-hmC residues, which trigger an ELISA-like reaction that allows colorimetric quantification at 450 nm.

### 2.7. miRNA Expression Array and Validation by Single Real-Time PCR

For microRNA (miRNA) expression array, total RNA and miRNA were extracted employing the miRNeasy Mini Kit (Qiagen) according to the manufacturer's instructions. The yield, purity and quality of the samples were determined by the A260/280 ratio in a NanoDrop® ND-1000 apparatus (Thermo Scientific). RNA samples from 24 females (n=6 per group) were converted into cDNA through a Reverse Transcription (RT) reaction using the miRCURY™ LNA™ miRNA RT Kit (Exiqon) according to the manufacturer's instructions. The expression of 22 mature miRNAs was then analysed using Mouse Pick&Mix miRNA PCR panel (Exiqon) (Supplementary Table 3 and 4). miRNA expression was measured in a StepOnePlus Real-Time PCR system (Applied Biosystems).

SYBR Green-based real-time PCR was performed on the detection system StepOnePlus (Applied Biosystems) for miRNA expression. In compliance with the miRCURY LNA™ SYBR Green PCR Kit Protocol (Qiagen), each reaction mixture contained 4,5µL of SYBR Green PCR Master Mix (2X), 0,5µL of ROX, 3µL of product from RT reaction diluted 1:60, 1µL of nuclease-free water and 1µL of miRNA probes (Exiqon) (Supplementary Table 2). Data were analysed using the comparative cycle threshold (Ct) method in which the SNORD68 small non-coding RNA transcript level was employed to normalize differences, since it presented similar expression level between groups. Each sample was analysed in duplicate and results represent the n-fold difference of the transcript levels among different groups.

### 2.8. Oxidative Stress Determination

Hydrogen peroxide was measured in hippocampus protein homogenates as an indicator of oxidative stress, and it was quantified using the Hydrogen Peroxide Assay Kit (Sigma-Aldrich, St. Louis, MI) according to the manufacturer's instructions.

### 2.9. Data analysis

Data analysis was conducted using GraphPad Prism ver. 7 statistical software. Data are expressed as the mean ± standard error of the mean (SEM) of at least 6 samples per group. Diet and treatment effects were assessed by the Two-Way ANOVA analysis of variance, followed by Tukey post-hoc analysis or two-tail Student's t-test when it was necessary. Statistical significance was considered when *p*-values were <0.05. The statistical outliers were determined with Grubbs' test and subsequently removed from the analysis when necessary.

## 3. Results

### 3.1. Epigenetic modulation triggers compacted chromatin after Chronic Mild Stress

In attempting to systematically address which are the epigenetic modifications caused by chronic mild stressful stimuli, we studied the main major epigenetic marks that include histone modifications, DNA methylation and non-coding RNAs.

Regarding histone modifications, we studied global histone 3 (H3) and histone 4 (H4) acetylation, phosphorylation of histone 2A (H2A.X) protein levels, methylation of H3 acetylated at Lys9 protein levels, as well as, several deacetylases gene expression and/or protein levels, such as HDAC2, Sirt1, Sirt2 and Sirt6. CMS decreased H3 acetylation in senescence-resistant mice, similarly to SAMP8 Control group, and increased in SAMP8 mice (Fig. 1 A). Considering H4, no statistically significant differences were determined, although a tendency to diminish in SAMR1 was observed (Fig. 1 B). On one hand, in accordance to H3 acetylation levels, there was a huge difference in histone deacetylase 2 (HDAC2) protein levels between SAMR1 and SAMP8 Control groups, being higher in SAMP8 (Fig. 1 C). On the other hand, CMS modified HDAC2 protein levels, concretely decreased in SAMP8 and increased in

SAMR1 compared to their littermates. Other deacetylases enzymes are sirtuins (Sirt) family. Not only gene expression (Fig 1 D-E), but also protein levels of Sirt1, Sirt2 and Sirt6 were clearly decreased in SAMP8 mice compared to their control strain (SAMR1). In addition, CMS reduced *Sirt1* (Fig. 1 D) and *Sirt2* (Data not shown) gene expression and protein levels (Data not shown) in SAMR1 mice, but not in SAMP8. Moreover, histones can suffer different modifications such as phosphorylation or methylation, among others. In our hands, p-H2A-X protein levels did not differ between SAMR1 and SAMP8 Control groups. Methylation of H3K9 was also higher in SAMP8 (Fig. 1 G). Of note, CMS increased phosphorylated form of histones p-H2A-X and methylation of H3K9 in SAMP8 in reference their control littermates, as well as, compared to stressed SAMR1 (Fig. 1 F-G).

Considering DNA methylation, global 5-mC DNA was slightly lower in SAMP8 compared to SAMR1. CMS significantly reduced global methylation both in SAMP8 and SAMR1 (Fig. 1 H). DNA methylation occurs through DNA MethylTransferase (DNMT) enzymes, of which DNMT1, DNMT3A and DNMT3B are the best characterized. As described, DNMTs were significant highly expressed in SAMP8 compared to SAMR1 Control group in CMS animals (Fig. 2 B for *Dnmt3,* Data not shown for *Dnmt1* and *Dnmt2*). 5-mC can be further oxidized to 5-hydroxymethyl-cytosine (5-hmC) due to ten-eleven translocase (TET) enzymes. SAMP8 mice had lower 5-hmC levels than SAMR1 mice (Fig. 1 I). Accordingly, TET2 protein levels were lower in SAMR1 than in SAMP8. CMS reduced TET2 protein levels in SAMR1 up to levels observed in SAMP8 Control group (Fig. 1 J).

miRNA also play an important role in regulating gene expression. Thereby we decided to perform a microarray with 84 miRNAs related with neurodegeneration and aging in order to evaluate the influence of our experimental conditions (strain and CMS) those miRNA expression. Considering these results (Supplementary Table 3 and 4), we proceeded to validate the relative expression of those modified miRNA in a significant manner regarding strain and CMS (Supplementary Figure 1).

miR-29c is involved in neural proliferation regulation by Dnmt3. Although no statistical differences were seen, it seems that SAMP8 have higher relative expression than SAMR1 and CMS contributed to increase it (Fig. 2 A-B). Those changes correlate with the tendencies seen in miR-29c-3p relative expression. miR-431-5p, miR-298-5p, miR-98-5p and miR-140-5p expression were lower in SAMP8 than in SAMR1 (Fig. 2 C,E,G,I). Those miRNA are related to inhibition of neurodegenerative pathways, its expression diminution correlated with changes in effector protein expression as β-catenin, β-site APP Cleaving Enzyme 1 (BACE1), soluble amyloid precursor protein-β (sAPPβ) and A Disintegrin and Metalloproteinase Domain-containing protein 10 (ADAM10) (Fig. 2 D,F,H,J). Furthermore, CMS seemed to reduce miR-431-5p expression in SAMR1 group, although not statistical differences were observed (Fig. 2 C-D). miR-181a-5p expression was higher in SAMP8 than SAMR1 (Fig 2 K). Mammalian Target Of Rapamycin Complex 1 (mTORC1) is targeted by this miRNA, regulating cell growth, proliferation and survival. Likewise, mTORC1 protein levels were significant higher in SAMP8 than in SAMR1 mice (Fig. 2 L). Stressful stimuli only increased miR-181a-5p relative expression in SAMR1 mice compared to their control littermates but not in SAMP8 (Fig. 2 K). Correlating with miRNA expression, SAMR1 stressed group showed higher protein levels than SAMR1 Control (Fig. 2 L). BCL2 protein levels are controlled by miR-106b-5p. SAMP8 mice showed higher relative expression in comparison with SAMR1 animals and CMS reduced its expression only in SAMP8 strain (Fig. 2 M), which correlated with BCL2 protein levels (Fig. 2 N).

### 3.2. Chronic Mild Stress attenuates antioxidant defence mechanisms

As mentioned before, CMS modulated cell oxidative stress mechanisms favouring an oxidative state. SAMP8 animals showed higher $H_2O_2$ levels in the hippocampus than SAMR1 groups, as well as reduced protein levels of the antioxidant enzymes superoxide dismutase (SOD), catalase (CAT) and glutathione peroxidase (GPX1), suggesting impaired mechanisms to fight against OS (Fig. 3 A-E). CMS induced a diminution in Nuclear factor erythroid 2-related factor 2 (NRF2) protein levels only in SAMR1, but reduced antioxidant enzymes studied in both strains. In addition, CMS produced a slight but not significant tendency to increase aldehyde oxidase 1 (*Aox1*) gene expression, a pro-oxidant enzyme, in both strains (Fig. 3 F).

### 3.3. Inflammatory activation is induced after application of Chronic Mild Stress

SAMP8 mice show higher protein levels of NF-κB compared to SAMR1 Control group. CMS promoted higher cytokines expression in SAMR1 than in SAMP8, as showed in the ratio *Interleukin(Il)-6/Il-10* and *tumor necrosis factor (Tnf) α* levels (Fig. 4 A-C), although not statistical differences were found. In accordance, *Glial fibrillar acidic protein (Gfap)* gene expression increased in both CMS groups in comparison to respective controls (Fig. 4 D).

### 3.4. Chronic Mild Stress modulates APP processing as well as alters microtubule stabilization through hyperphosphorylation of Tau protein

Observing the results, SAMP8 showed lower ADAM10 protein levels than SAMR1 animals. CMS promoted β-amyloid amyloidogenic pathway in SAMR1 mice, increased sAPPβ protein levels, increased Aβ-precursor gene expression and BACE1 protein levels as well as reduced ADAM10 protein levels (Fig. 2 F, H, J; 5 A).

SAMP8 had higher Ser396 p-Tau levels (Fig. 5 B-C) than SAMR1. Similarly, GSK-3β phosphorylation at Ser9 protein level was higher in SAMP8 in reference to SAMR1 (Fig. 5 D). CMS increased tau hyperphosphorylation at Ser396 and Ser404 compared to control groups; surprisingly, CMS reduced GSK-3β protein levels (Fig. 5 D).

### 3.5. Chronic Mild Stress promotes cell clearance through autophagy activation

Because autophagy has a key role in neurodegeneration, we evaluated Beclin 1, microtubule-associated protein 1A/1B-Light Chain 3 (LC3B), B-Cell Lymphoma 2 (BCL2) and mammalian Target Of Rapamycin (mTOR). Beclin 1 and LC3B protein levels were lower in SAMP8 than in SAMR1, whereas mTOR activation, measured by p-mTOR/mTOR ratio was higher in SAMP8 mice. CMS decreased pro-autophagic protein levels studied (Beclin 1 and LC3B) in SAMR1 mice, as well as there was a slight increase in mTOR activation. By contrast, in SAMP8 animals, stressful stimuli increased autophagy markers evaluated (Fig. 6 A-C; 2 N).

### 3.6. Anxiety-like behaviour, memory decline and poorer cognitive abilities after Chronic Mild Stress

As mentioned, stress produced behavioural changes in animals. Concretely, the CMS treatment applied to animals contributed to increase locomotor activity in both mice strains, indicating that anxiety sensation and escape desire increased (Fig. 7 A). Regarding the other parameters evaluated in the OFT, SAMR1 travelled more distance and stood longer in the centre compared to SAMP8, although there were no statistically significant differences. In addition, CMS reduced those parameters in both strains compared to control animals (Fig. 7 B-D). Among these parameters indicating anxious behaviour were grooming and rearing. CMS treated groups showed higher number of rears and lower number of grooms than their controls (Fig. 7 E-F).

Referring to memory, we evaluated the recognition and spatial memory as well as learning abilities, through MWM and NORT. On one hand, there was a clear difference between strains because SAMP8 groups showed lower recognition memory than SAMR1 mice. On the other hand, MWM learning curves demonstrated that all mice learned where was the platform during the training days, as the time to reach the platform and the distance travelled was lower than the first day (Fig. 7 I-J). CMS treatment reduced recognition memory at both, short- and long-term (2h and 24h) (Fig. 7 G-H). Considering results obtained in MWM, SAMR1 animals crossed more times the platform zone and its quadrant than SAMP8 mice, as well as they stood and swum more distance in the platform zone (Fig 7. K-M) indicating a significantly better performance in this maze from SAMR1 than SAMP8. CMS decreased the value of those parameters in SAMR1 bringing them closer to SAMP8 values, although did not reach significance. Overall, results obtained in MWM and in accordance to OFT results indicated that CMS increased the total distance travelled during the training in comparison with Control groups.

Lastly, glucose metabolism was evaluated through glucose tolerance test. SAMP8 mice showed higher glucose area under the curve than SAMR1 mice, although this relation was upside down between animals that received CMS (Fig. 7 N), suggesting that stressed SAMR1 mice develop a sugar metabolism similar to SAMP8 animals.

## 4. Discussion

Understanding the mechanisms that define aging and differentiate what determines whether it is pathologic or healthy is one of the challenges that science has faced in recent years. Life expectancy has increased and so the number of older people. In addition, the life rhythm has changed becoming increasingly stressful. It has been shown that the environment is extremely important in the development of several diseases, compromising healthy aging; concretely, stressful lifestyle has been identified as an important risk factor for cognitive decline. Therefore, it is crucial to study the effects of stress on cognition and its relationship with aging in order to unveil what challenges we might have to cope with as a society in a not so far future. We hypothesize that chronic stress would modulate a large constellation of cellular mechanisms implied in aging and age-related neurodegenerative pathologies.

During aging, there are several epigenetic mechanisms altered, which include DNA methylation, histone modifications, nucleosome remodelling and miRNA-mediated gene regulation [2,26]. In the present study, we evaluated three main epigenetic marks, which modulate chromatin structure and act as platforms for recruitment, assembly or retention of chromatin-associated factors: histone posttranslational modifications, DNA methylation and miRNA-mediated gene regulation. One of the posttranslational modifications of histones is acetylation. This process removes histone positive charge; thereby the condensed chromatin (heterochromatin) is transformed into a more relaxed structure (euchromatin) that is associated with greater levels of gene transcription [27,28]. However, chromatin condensation depends on different processes including methylation and histone deacetylation. This last process is due to histone deacetylases (HDAC) enzymes. Deregulation of histone acetylation has been related to increase the risk of age-dependent memory impairment in mice [4,29,30]. Specifically, histone H4 lysine 12 acetylation alterations causes impaired memory consolidation as well as its restoration reinstates the expression of learning-induced genes and in consequence, cognitive abilities [29]. In accordance to Cosín-Tomás [31], we found that CMS increased HDAC2 protein levels only in SAMR1 females, similarly to SAMP8 Control mice, which lead us to hypothesize that acetylated histone protein

levels were diminished. This was confirmed evaluating acetylated H3 and H4 protein levels. However, while stress produced changes in H3 acetylation, these changes were not observed in H4. Nevertheless, the decrease in H3 acetylation in SAMR1 mice under CMS, similarly to not stressed SAMP8 was correlated with changes on cognition. Other HDACs include sirtuins family; however, it is worth noting that several members of this family do not have deacetylase activity [32]. Sirt have been linked to aging as they modulate genomic stability, stress resistance and energy metabolism. Activation of Sirt1 enables the deacetylation of a variety of proteins, resulting in a robust, protective cellular response, as it regulates processes such as cell death, metabolism or neurodegeneration [33]; while Sirt2 has been reported to regulate oxidative stress, genome integrity and myelination and its dysfunction is found in most of age-related neurodegenerative disorders such as AD, Parkinson's disease or Amyotrophic Lateral Sclerosis, as well as in physiological aging [34]. Accumulated evidence indicates that *Sirt6* gene expression is lower in the hippocampus and cerebral cortex of aged mice [35,36] and that it is concerned with H3K9 acetylation [35]. In reference to this family of deacetylases our results demonstrate decreased *Sirt1, Sirt2* and *Sirt6* gene expression in SAMP8 mice compared to SAMR1 and to SAMR1 under CMS. Compelling evidence has proposed that methylation of lysine 9 of histone 3 (H3K9) promotes DNA methylation maintenance in mammals and is a hallmark of heterochromatin formation and subsequent gene silencing [2,37,38]. As with histone phosphorylation, CMS treatment increased H3K9 methylation in SAMP8 animals but not in SAMR1 suggesting that even they showed more H3 acetylation, also resulted in more methylation. Therefore, we demonstrate that CMS favoured chromatin condensation and in consequence, promoted gene silencing.

In reference to other modifications, histone phosphorylation belongs to the cellular response to DNA damage, as phosphorylated histone H2A.X demarcates large chromatin domains around the site of DNA breakage [2]. Additionally, multiple studies have also shown that histone phosphorylation plays crucial in other nuclear processes, such as DNA replication because of apoptosis or DNA damage [39]. Here CMS raised phosphorylated H2A.X protein level in senescence-accelerated but not in senescence-resistant mice, suggesting that stressful stimuli activate repair/survival mechanisms

rather than apoptotic response in SAMP8 mice but not in SAMR1. As two major mechanisms for epigenetic regulation, DNA methylation and histone modifications must act coordinately [37]. It is well known that DNA methylation at the fifth position of cytosine (5-mC) plays an important role in neuronal gene expression and neural development. Several studies support the idea that dysregulated DNA methylation/demethylation is linked to many neuronal disorders, including AD onset and progression; however, the relationship between AD and altered 5-mC levels is not known [40]. 5-mC can be further oxidized to 5-hmC, among others, by the TET family of dioxygenases. 5-mC and 5-hmC exert opposite effects on gene expression; the former is general associated with gene silencing, whereas the latter is mainly involved in up-regulation of gene expression [41]. In this study, stressful environment produced lower 5-mC in both mice strains and differences between strains were observed in 5-hmC marker. Accordingly, TET2 protein levels differed between SAMR1 and SAMP8 animals. Despite our previous results, conversely 5-mC and 5-hmC results appear to contradict the transcriptional access to DNA, but as is known the term global DNA methylation describes this process across the entire genome and does not represent a precise landscape for specific transcriptional activity; however, global methylation determination is useful as it provides an over-arching picture of methylation status, it is misleading which genes show altered DNA methylation and which do not [42].

Furthermore, we evaluated expression changes of miRNAs related to oxidative stress, AD neurophatological hallmarks, autophagy and neurodegeneration. Of 22 miRNA evaluated, those that presented statistically significant changes under experimental conditions were further validated and target genes studied (Supplementary Figure 1). Firstly, we studied miR-29c relative expression, which is involved in neural proliferation regulation through Dnmt3a. *Dnmt3a* expression was higher in SAMP8 compared to SAMR1 mice correlating with miR-29c-3p gene expression. In our hands CMS slightly contributed to change *Dnmt3a* expression in mice, being increased in SAMR1. Because, recent studies demonstrate that DNMT inhibitors provided neuroprotection in cellular cultures [43,44], the increase in *Dnmt3a* induced by CMS could mean a deleterious effect on SAMR1 health.

Considering AD neuropathology, we studied miR-431-5p, miR-298-5p, miR-98-5p and miR-140-5p. It has been described that miR-431-5p cooperates with DKK1 to inhibit Wnt/β-catenin pathway. SAMP8 showed lower relative expression of this miRNA in comparison to SAMR1 mice; changes in β-catenin protein levels were in line with miR-431-5p. Furthermore, CMS reduced mildly miR-431-5p gene expression and β-catenin protein levels in SAMR1. β-catenin is regulated by GSK-3β activity, depending on its phosphorylation. As reported, GSK3-β inactive form (Ser9 phosphorylated) protein levels were lower in SAMP8 in reference to SAMR1 [33], and also CMS decreased them, especially in SAMP8. It is known that GSK3-β activity is associated with AD neuropathology as it exacerbates cognitive impairment [45]. In fact, higher activity of this kinase has been found in AD patients and its inhibition restores spatial memory deficits, reduces tau hyperphosphorylation and decreases reactive gliosis and neuronal death in rodents [45]. Furthermore, it has been described that GSK3-β inhibition reduces BACE1-mediated cleavage of APP through NF-κB signalling-mediated mechanism, so that it reduces β-amyloid pathology [46]. Accordingly, we found that CMS increased Ser396 and Ser404 Tau hyperphosphorylation, most pronounced in SAMP8, and promoted amyloid precursor protein (APP) gene expression in both mice strains. In fact, APP processing is regulated by miR-298-5p, which in turn regulates BACE1. miR-298-5p expression differed between SAMR1 and SAMP8 animals, in contrast with BACE1 protein levels. It is reported that BACE1, sAPPβ and β-CTF protein levels were increased when miR-98-5p up-regulated. CMS increased miR-98-5p relative expression and sAPPβ in SAMR1 compared to the Control group, but not in SAMP8. However as mentioned, BACE1 was not modulated under CMS. Taking into account that BACE1 can be up- or down-regulated by different miRNAs, discrepancies can be explained by compensatory responses among different signals. ADAM10 protein levels are controlled by miR-140-5p. Again, huge differences in miR-140-5p gene expression and ADAM10 protein levels were observed between strains. Differences were between mice under CMS in SAMR1 but not in SAMP8.

miR-181a-5p is involved in regulation of cell growth, proliferation and survival through mTOR complex 1 (mTORC1) and downstream pathway, which protein levels were increased in SAMP8 in comparison to SAMR1 mice. In addition, stressful stimuli

increased miR-181a-5p relative expression in SAMR1 mice compared to their control littermates and no changes were observed between SAMP8 animals. By contrast, CMS groups, in both strains, showed higher mTORC1 protein levels than respective control littermates. Lastly, BCL2 protein levels were controlled by miR-106b-5p. SAMP8 mice had higher miR-106b-5p compared to SAMR1, but no changes were found in BCL2 protein levels. CMS reduced miR-106b-5p gene expression, increasing BCL2 protein levels in SAMP8, without affecting SAMR1 strain.

Autophagy declines during aging, so that it may contribute to the deleterious accumulation of aberrant proteins observed in aged cells. Interestingly, failure of this process has been reported to worsen aging-associated diseases, such as neurodegeneration or cancer [18]. Pro autophagic proteins such as Beclin1 and LC3B became decreased after CMS treatment and in concordance p-mTOR ratio was increased. Moreover, we demonstrate huge differences between SAMR1 and SAMP8 Control groups, indicating a reduced autophagic flux in senescent mice. CMS induced impairment in autophagy was more robust and consistent in SAMR1 than in SAMP8, supporting the hypothesis that CMS accelerates the senescence process.

Following the same line about overall processes linked to senescence, it has been widely described that OS possesses a pre-eminent role in pathological senescence and the pathogenesis of AD. In general, cells possess antioxidant mechanisms to cope with OS, such as GPX, Catalase and SOD, among others; which in turn are regulated by Nrf2 transcriptional pathway. Herein we found that mice under CMS had lower NRF2 protein levels than control groups and this in turn could explain the lowest protein levels of antioxidant defence as GPX1, SOD1 and Catalase. Consistent with this, CMS promoted an increase in the pro-oxidant enzyme *Aox1* gene expression and higher accumulation of ROS. Noteworthy, as described, differences between strains were found in most of the markers evaluated [4].

As far as aging and AD are concerned, dysregulation of inflammatory mediators and astrogliosis are major culprits in the development of chronic inflammation and the immunosenescence process, as well as are related to cognitive decline and progression

Peer-reviewed version available at Int. J. Mol. Sci. 2020, 21, 1154; doi:10.3390/ijms21031154

of neurodegenerative diseases [15]. For instance, our results demonstrate significant increase in protein levels for NF-κB, transcription factor regulating pro-inflammatory signals, in SAMP8 mice in comparison with SAMR1. In accordance to Chung et al. [15], *Il-6* and *TNF-α* gene expression were up regulated in SAMP8 mice. Interestingly CMS increased proinflammatory pathways in SAMR1 but not in SAMP8. Moreover, we found an increase in *Gfap* gene expression in SAMR1 CMS compared to SAMR1 Control group. In accordance, recently it has been described that modulating astrogliosis enhances AD pathology in mice [47].

It is widely accepted the detrimental effect of stress on psychological well-being and cognitive functioning, emphasizing the relationship between stress and memory. It is noteworthy that chronic stress signs underlie some of the characteristics described in cognitive decline, either in aging or in neurodegenerative diseases, such as AD [19,48]. It has been stated that epigenetic machinery is essential for cognitive function [2,29,49]. Likewise, DNA methylation influences hippocampal memory formation and growing evidence suggests that the modulation of epigenetic processes by stress, EE and/or hormones is key in regulating memory function.

In line with molecular results presented, behavioural changes induced by CMS were explored in SAMP8 and SAMR1 mice. Results obtained point out that not only a stressful environment triggers anxiety-like behaviour, but also it mitigates cognitive performance. Locomotor activity, the distance travelled in the central zone and other parameters indicating well-being/discomfort were altered in mice under CMS. Regarding recognition memory, clear differences were found between the different strains, although we can also assert a detrimental effect caused by CMS, especially on long-term memory. In agreement with these results, learning abilities and spatial memory in SAMR1 and SAMP8 at 6 months of age were significatively different and were negatively affected by the presence of chronic stressors. While stressful situations, glucose levels increase in order to have enough energy available to cope with stress. Aberrant glucose metabolism potentiates the aging phenotype and contributes to early stage central nervous system pathology [50]. According to

previous works, we found differences on blood glucose levels due to stress in SAMR1 mice, exhibiting similar glucose tolerance to SAMP8 Control mice.

## 5. Conclusion

Overall, CMS treatment produces detrimental effects in SAM female mice, such as inflammatory signalling activation, loss of antioxidant defence mechanisms, changes in behaviour and reduced cognitive abilities (Fig. 8). Interestingly, CMS promoted significant epigenetic and biochemical changes in SAMR1 animals, a normal mice strain, driving them to an aging-specific phenotype represented by SAMP8 mice, a senescence mice model, in which the negative effects of CMS are probably limited because its senescence level is already elevated.

## 6. Acknowledgements

This study was supported by Ministerio de Economía y Competitividad of Spain and FEDER (SAF2016-77703) and 2017SGR106 (AGAUR, Catalonia). Financial support was provided for D.P.I. (FPU program).

## 7. References

1. Cristòfol, R.; Porquet, D.; Corpas, R.; Coto-Montes, A.; Serret, J.; Camins, A.; Pallàs, M.; Sanfeliu, C. Neurons from senescence-accelerated SAMP8 mice are protected against frailty by the Sirtuin 1 promoting agents melatonin and resveratrol. *J Pineal Res* **2012**, *52*, 271-281.

2. Harman, M.F.; Martín, M.G. Epigenetic mechanisms related to cognitive decline during aging. *J Neuro Res* **2019**, *00*, 1-13.

3. Guerreiro, R.; Bras, J. The age factor in Alzheimer's disease. *Genome Medicine* **2015**, *7*, 106.

4. Griñan-Ferré, C.; Puigoriol-Illamola, D.; Palomera-Ávalos, V.; Pérez-Cáceres, D.; Companys-Alemany, J.; Camins, A.; Ortuño-Sahagún, D.; Rodrigo, M.T.; Pallàs, M. Environmental Enrichment Modified Epigenetic Mechanisms in SAMP8 Mouse Hippocampus by Reducing Oxidative Stress and Inflammaging and Achieving Neuroprotection. *Front. Aging Neurosci.* **2016**, *8*, 241.

5. Sun, H.; Kennedy, P.; Nestler, E. Epigenetics of the Depressed Brain: Role of Histone Acetylation and Methylation. *Neuropsychopharmacol* **2013**, *38*, 124-137.

6. Turecki, G.; Meaney, M.J. Effects of the Social Environment and Stress on Glucocorticoid Receptor Gene Methylation: A Systematic Review. *Biol Psychiatry* **2016**, *79* (2), 87-96.

7. Sandi, C. Stress and Cognition. *WIREs Cogn Sci* **2013**, *4*, 245-261.

8. Wang, S.E.; Ko, S.Y.; Jo, S.; Jo, H.; Han, J.; Kim, Y.; Son, H. Downregulation of SIRT2 by Chronic Stress Reduces Expression of Synaptic Plasticity-related Genes through the Upregulation of Ehmt2. *Exp Neurobiol.* **2019**, *28 (4)*, 537-546.

9. Borcel, E.; Pérez-Alvarez, L.; Herrero, A.I.; Brionne, T.; Varea, E.; Berezin, V.; Bock, E.; Sandi, C.; Venero, C. Chronic stress in adulthood followed by intermittent stress impairs spatial memory and the survival of newborn hippocampal cells in aging animals: prevention by FGL, a peptide mimetic of neural cell adhesion molecule. *Behav Pharmacol.* **2008**, *19 (1)*, 41-9.

10. Rahman, M.M.; Callaghan, C.K.; Kerskens, C.M.; Chattarji, S.; O'Mara, S.M. Early hippocampal volume loss as a marker of eventual memory deficits caused by repeated stress. *Sci. Rep.* **2016**, *6*, 29127.

11. Jett, J.D.; Bulin, S.E.; Hatherall, L.C.; McCartney, C.M.; Morilak, D.A. Deficits in cognitive flexibility induced by chronic unpredictable stress are associated with impaired glutamate neurotransmission in the rat medial prefrontal cortex. *Neurosci.* **2017**, *346*, 284-297

12. Justice, N.J. The relationship between stress and Alzheimer's disease. *Neurobiol Stress.* **2018**, *8*, 127-133.

13. Bisht, K.; Sharma, K.; Tremblay, M. Chronic stress as a risk factor for Alzheimer's disease: Roles of microglia-mediated synaptic remodeling, inflammation, and oxidative stress. *Neurobiol Stress.* **2018**, *9*, 9-21.

14. Griñán-Ferré, C.; Corpas, R.; Puigoriol-Illamola, D.; Palomera-Ávalos, V.; Sanfeliu, C.; Pallàs, M. Understanding Epigenetics in the Neurodegeneration of Alzheimer's Disease: SAMP8 Mouse Model. *J Alzheimers Dis.* **2018**, *62(3)*, 943-963.

15. Chung, H.Y.; Kim, D.H.; Lee, E.K.; Chung, K.W.; Chung, S.; Lee, B.; Seo, A.Y.; Chung, J.H.; Jung, Y.S.; Im, E.; Lee, J.; Kim, N.D.; Choi, Y.J.; Im, D.S.; Yu, B.P. Redefining

Chronic Inflammation in Aging and Age-Related Diseases: Proposal of the Senoinflammation Concept. *Aging Dis.* **2019**, *10(2)*, 367-382.

16. Petersen, K.S.; Smith, C. Ageing-Associated Oxidative Stress and Inflammation Are Alleviated by Products from Grapes. *Oxidative Medicine and Cellular Longevity* **2016**, *2016*, 12.

17. Escobar, K.A.; Cole, N.H.; Mermier, C.M.; VanDusseldorp, T.A. Autophagy and aging: Maintaining the proteome through exercise and caloric restriction. *Aging Cell* **2019**, *18(1)*, e12876.

18. Gouras, G.K. Aging, Metabolism, Synaptic Activity, and Aβ in Alzheimer's Disease. *Front Aging Neurosci.* **2019**, *11*, 185.

19. Puigoriol-Illamola, D.; Griñán-Ferré, C.; Vasilopoulou, F.; Leiva, R.; Vázquez, S.; Pallàs, M. 11β-HSD1 Inhibition by RL-118 Promotes Autophagy and Correlates with Reduced Oxidative Stress and Inflammation, Enhancing Cognitive Performance in SAMP8 Mouse Model. *Mol Neurobiol.* **2018**, *55(12)*, 8904-8915.

20. Martinez-Lopez, N. Autophagy and Aging. *Adv Exp Med Biol.* **2015**, *847*, 73-87.

21. Takeda, T.; Hosokawa, M.; Higuchi, K. Senescence-Accelerated Mouse (SAM): A Novel Murine Model of Accelerated Senescence. *Journal of the American Geriatrics Society* **1991**, *39(9)*, 911-919.

22. Wang, J.; Yuan, J.; Pang, J.; Ma, J.; Han, B.; Geng, Y.; Shen, L.; Wang, H.; Ma, Q.; Wang, Y.; Wang, M. Effects of Chronic Stress on Cognition in Male SAMP8 Mice. *Cell Physiol Biochem* **2016**, *39*, 1078-1086.

23. Griñán-Ferré, C.; Pérez-Cáceres, D.; Gutiérrez-Zetina, S.M.; Camins, A.; Palomera-Avalos, V.; Ortuño-Sahagún, D.; Rodrigo, M.T.; Pallàs, M. Environmental Enrichment Improves Behavior, Cognition, and Brain Functional Markers in Young Senescence-Accelerated Prone Mice (SAMP8). *Mol Neurobiol.* **2015**, *53*, 2435-2450.

24. Puigoriol-Illamola, D.; Leiva, R.; Vázquez-Carrera, M.; Vázquez, S.; Griñán-Ferré, C.; Pallàs, M. 11β-HSD1 Inhibition Rescues SAMP8 Cognitive Impairment Induced by Metabolic Stress. *Mol Neurobiol.* **2019**, 1-15.

25. Vorhees, C.V.; Williams, M.T. Morris water maze: procedures for assessing spatial and related forms of learning and memory. *Nature protocols* **2006**, *1(2)*, 848-858.

26. Foster, J.A.; Rinaman, L.; Cryan, J.F. Stres & the gut-brain axis: Regulation by the microbiome. *Neuribiol Stress*. **2017**, *7*, 124-136.

27. Watson, J.D.; Baker, T.A.; Gann, A.; Levine, M.; Losik, R. *Molecular biology of the gene;* Pearson/CSH Press, 7th Ed.; Boston, USA, 2014.

28. Turner, B.M. Histone acetylation and an epigenetic code. *BioEssays* **2000**, *22(9)*, 836-45.

29. Peleg, S.; Sananbenesi, F.; Zovoilis, A.; Burkhardt, S.; Bahari-Javan, S.; Agis-Balboa, R.C.; Cota, P.; Wittnam, J.L.; Gogol-Doering, A.; Opitz, L.; Salinas-Riester, G.; Dettenhofer, M.; Kang, H.; Farinelli, L.; Chen, W.; Fischer, A. Altered histone acetylation is associated with age-dependent memory impairment in mice. *Science.* **2010**, *328(5979)*, 753-6.

30. Cuadrado-Tejedor, M.; Pérez-González, M.; García-Muñoz, C.; Muruzabal, D.; García-Barroso, C.; Rabal, O.; Segura, V.; Sánchez-Arias, J.A.; Oyarzabal, J.O.; Garcia-Osta, A. Taking Advantage of the Selectivity of Histone Deacetylases and Phosphodiesterase Inhibitors to Design Better Therapeutic Strategies to Treat Alzheimer's Disease. *Front. Aging Neurosci.* **2019**, *11*, 149.

31. Cosín-Tomás, M.; Alvarez-López, M.J.; Sanchez-Roige, S.; Lalanza, J.F.; Bayod, S.; Sanfeliu, C.; Pallàs, M.; Escorihuela, R.M.; Kaliman, P. Epigenetic alterations in hippocampus of SAMP8 senescent mice and modulation by voluntary physical exercise. *Front Aging Neurosci.* **2014**, *6*, 51.

32. Herskovits, A.Z.; Guarente, L. SIRT1 in neurodevelopment and brain senescence. *Neuron*. **2014**, *81(3)*, 471-83.

33. Pallàs, M. Senescence-Accelerated Mice P8: A Tool to Study Brain Aging and Alzheimer's Disease in a Mouse Model. *Cell Biology* **2012**, 12.

34. Fourcade, S.; Outeiro, T.F.; Pujol, A. SIRT2 in age-related neurodegenerative disorders. *Aging* **2018**, *10*.

35. Khan, R.I.; Nirzhor, S.S.R.; Akter, R. A Review of the Recent Advances Made with SIRT6 and its Implications on Aging Related Processes, Major Human Diseases, and Possible Therapeutic Targets. *Biomolecules* **2018**, *8(3)*, 44.

36. Jesko, H.; Wencel, P.; Strosznajder, R.P.; Strosznajder, J.B. Sirtuins and Their Roles in Brain Aging and Neurodegenerative Disorders. *Neurochem Res* **2017**, *42(3)*, 876-890.

37. Zhao, Q.; Zhang, J.; Chen, R.; Wang, L.; Li, B.; Cheng, H.; Duan, X.; Zhu, H.; Wei, W.; Li, J.; Wu, Q.; Han, J-D.J.; Yu, W.; Gao, S.; Li, G.; Wong, J. Dissecting the precise role of H3K9 methylation in crosstalk with DNA maintenance methylation in mammals. *Nat Commun* **2016**, *7*, 12464.

38. Palmer, J.M.; Perrin, R.M.; Dagenais, T.R.; Keller, N.P. H3K9 methylation regulates growth and development in Aspergillus fumigatus. *Eukaryot Cell* **2008**, *7(12)*, 2052-60.

39. Rossetto, D.; Avvakumov, N.; Côte, J. Histone phosphorylation: a chromatin modification involved in diverse nuclear events. *Epigenetics* **2012**, *7 (10)*, 1098-108.

40. Fetahu, I.S.; Ma, D.; Rabidou, K.; Argueta, C.; Smith, M.; Liu, H.; Wu, F.; Shi, Y.G. Epigenetic signatures of methylated DNA cytosine in Alzheimer's disease. *Sci Adv* **2019**, *5(8)*, eaaw2880.

41. Sherwani, S.I.; Khan, H.A. Role of 5-hydroxymethylcytosine in neurodegeneration. *Gene* **2015**, *570(1)*, 17-24.

42. Yokoyama, A.S.; Rutledge, J.C.; Medici, V. DNA methylation alterations in Alzheimer's disease. *Environ Epigenet.* **2017**, *3(2)*, dvx008.

43. Chestnut, B.A.; Chang, Q.; Prince, A.; Lesuisse, C.; Wong, M.; Martin, L.J. Epigenetic regulation of motor neuron cell death through DNA methylation. *J Neurosci.* **2011**, *31*, 16619-16636.

44. Hernandez, D.G.; Nalls, M.A.; Gibbs, J.R.; Arepalli, S.; van der Brug, M.; Chong, S.; Moore, M.; Longo, D.L.; Cookson, M.R.; Traynor, B.J.; Singleton, A.B. Distinct DNA methylation changes highly correlated with chronological age in the human brain. *Hum Mol Genet* **2011**, *20(6)*, 1164-72.

45. Llorens-Martín, M.; Jurado, J.; Hernández, F.; Avila, J. GSK-3β, a pivotal kinase in Alzheimer disease. *Front Mol Neurosci.* **2014**, *7*, 46.

46. Ly, P.T.T.; Wu, Y.; Zou, H.; Wang, R.; Zhou, W.; Kinoshita, A.; Zhang, M.; Yang, Y.; Cai, F.; Woodgett, J.; Song, W. Inhibition of GSK-3β-mediated BACE1 expression reduces Alzheimer-associated phenotypes. *J Clin Invest.* **2013**, *123(1)*, 224-235.

47. Reichenbach, N.; Delekate, A.; Plescher, M.; Schmitt, F.; Krauss, S.; Blank, N.; Halle, A.; Petzold, G.C. Inhibition of Stat3-mediated astrogliosis ameliorates pathology in an Alzheimer's disease model. *EMBO Mol Med.* **2019**, *11(2)*, e9665.

48. Turner, K.; McCarthy, V.L. Stress and anxiety among nursing students: A review of intervention strategies in literature between 2009 and 2015. *Nurse Educ Pract*. **2017**, *22*, 21-29.

49. Stilling, R.M.; Fischer, A. The role of histone acetylation in age-associated memory impairment and Alzheimer's disease. *Neurobiol Learning Memory* **2011**, *96(1)*, 19-26.

50. Currais, A.; Prior, M.; Lo, D.; Jolivalt, C.; Schubert, D.; Maher, P. Diabetes exacerbates amyloid and neurovascular pathology in aging-accelerated mice. *Aging Cell* **2012**, *11*, 1017-1026.

**Figure 1.** Representative Western Blot for the ratio of Acetylated at Lys9 H3 protein levels and quantification (A), the ratio of Acetylated at Lys 12 H4 protein levels and quantification(B), HDAC2 protein levels and quantification (C), the ratio of p-H2A.X protein levels and quantification (F), the ratio of H3K9me2 protein levels and quantification (G) and TET2 protein levels and quantification (J). Relative gene expression of *Sirt1* (D) and *Sirt6* (E). Global 5-methylated cytosine (H) and 5-hydroxymethylated cytosine levels (I). Gene expression levels were determined by real-time PCR. Values in bar graphs are adjusted to 100% for protein levels of SAMR1 Control (R1 Ct). Values are mean ± Standard error of the mean (SEM); (n = 4 for each group). *p<0.05; **p<0.01; ***p<0.001; ****p<0.0001.

**Figure 2.** Validation of a representative subset of miRNA involved in the brain aging, neurodegeneration and autophagy. Relative expression of miR-29c-3p, miR-431-5p, miR-298-5p, miR-98-5p, miR-140-5p, miR-181a-5p and miR-106b-5p in the hippocampus of SAMR1 and SAMP8 mice (A, C, E, G, I, K, M). Relative gene expression of *Dnmt3a* (B) and representative Western Blot for β-Catenin protein levels and quantification (D), BACE1 protein levels and quantification (F), sAPPβ protein levels and quantification (H), ADAM10 protein levels and quantification (J), mTORC1 protein levels and quantification (L) and BCL2 protein levels and quantification (N). Gene expression levels were determined by real-time PCR. Values in bar graphs are adjusted to 100% for protein levels of SAMR1 Control (R1 Ct). Values are mean ± Standard error of the mean (SEM); (n = 6 for each group in miRNAs validation; n=4 for each group in WB and real-time PCR studies). *p<0.05; **p<0.01.

**Figure 3.** Representative OS measured as hydrogen peroxide concentration in homogenates of hippocampus tissue (A). Representative Western Blot for NRF2 protein levels and quantification (B), GPX1 protein levels and quantification (C), SOD1 protein levels and quantification (D), and Catalase protein levels and quantification (E). Relative gene expression of *Aox1* (F). Values in bar graphs are adjusted to 100% for protein levels of SAMR1 Control (R1 Ct). Gene expression levels were determined by real-time PCR. Values are mean ± Standard error of the mean (SEM); (n=4 for each group). *p<0.05; **p<0.01.

**Figure 4.** Representative Western Blot for NF-κB protein levels and quantification (A). Relative gene expression of *Il-6/Il-10* ratio, *Tnf-α* and *Gfap* (B-D). Values in bar graphs are adjusted to 100% for protein levels of SAMR1 Control (R1 Ct). Gene expression levels were determined by real-time PCR. Values are mean ± Standard error of the mean (SEM); (n=4 for each group). *p<0.05.

**Figure 5.** Relative gene expression of *Aβ-precursor* (A). Representative Western Blot for the ratio of pS396-Tau protein levels and quantification (B), the ratio of pS404-Tau protein levels and quantification (C) and the ratio of pS9-GSK-3β protein levels and quantification (D). Gene expression levels were determined by real-time PCR. Values in bar graphs are adjusted to 100% for protein levels of SAMR1 Control (R1 Ct). Values are mean ± Standard error of the mean (SEM); (n=4 for each group). *p<0.05; **p<0.01.

**Figure 6.** Representative Western Blot for Beclin 1 protein levels and quantification (A), the ratio of p-mTOR protein levels and quantification (B) and the ratio of LC3 protein levels and quantification (C). Values in bar graphs are adjusted to 100% for protein levels of SAMR1 Control (R1 Ct). Values are mean ± Standard error of the mean (SEM); (n=4 for each group). *p<0.05; **p<0.01; ***p<0.001.

**Figure 7.** Results of OFT for all mice groups. Locomotor Activity (A), Ratio of the distance travelled in the Center/Periphery zone (B), Time in the Center (C) and in the Periphery (D), number of Rearing (E) and number of Grooming (F). Results of NORT for all mice groups. Summary of DI from 2 and 24 hours after familiarization phase (G-H). Results of MWM for all mice groups. Learning curves of MWM during the spatial acquisition phase (I-J), number of Entries (K), Distance travelled (L) and Time (M) in platform zone during the test. Plasma levels of glucose 2g/kg intraperitoneal (i.p.) administration (N). Values are mean ± Standard error of the mean (SEM) (n=14 for each group). *p<0.05; **p<0.01; ***p<0.001; ****p<0.0001.

**Figure 8.** Flow chart of representative molecular pathways altered after Chronic Mild Stress

*Preprints* (www.preprints.org) | NOT PEER-REVIEWED | Posted: 21 January 2020 doi:10.20944/preprints202001.0244.v1

Peer-reviewed version available at *Int. J. Mol. Sci.* **2020**, *21*, 1154; doi:10.3390/ijms21031154

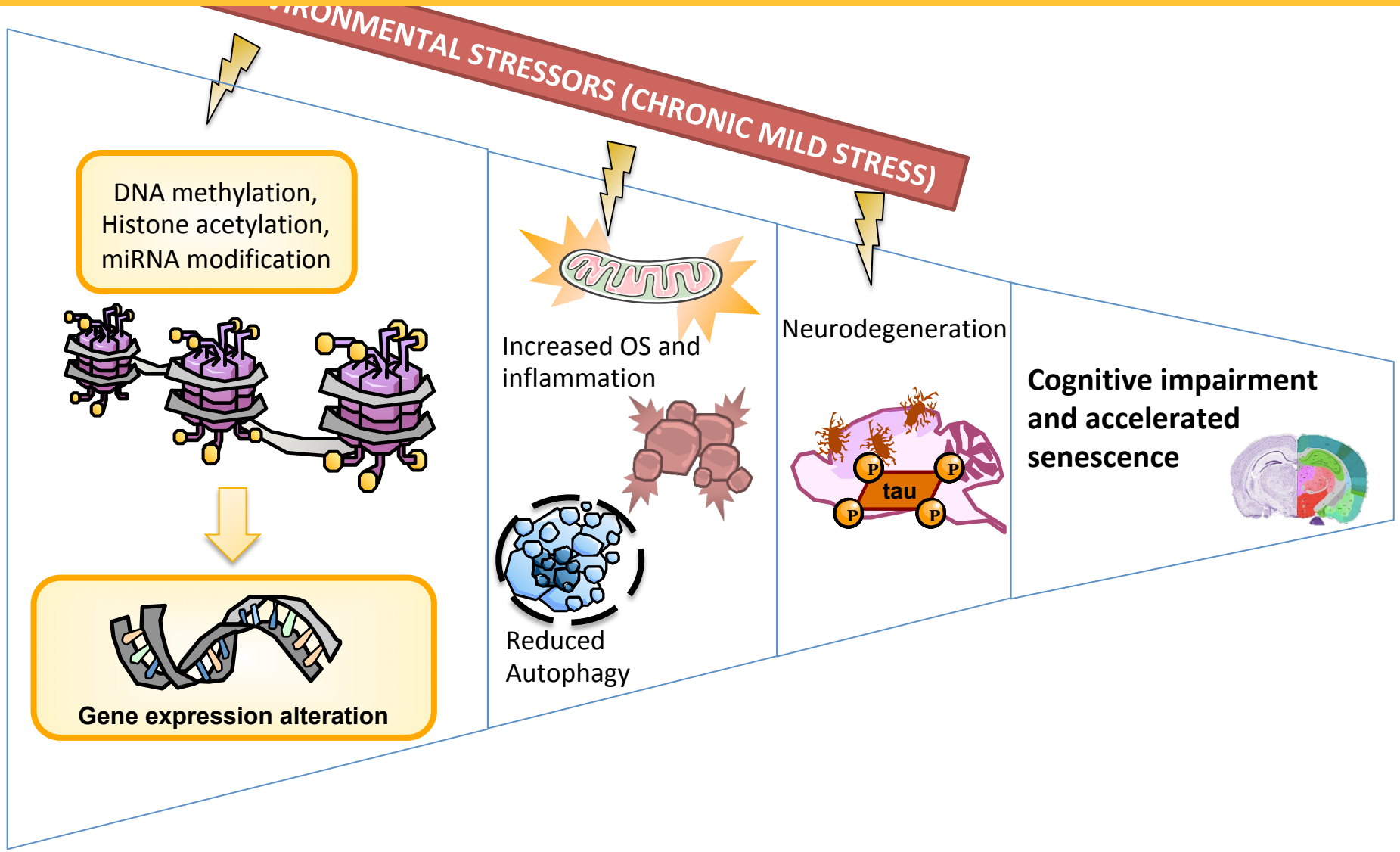

**Supplementary Table 1**. Antibodies used in Western blot studies.

| Antibody | Host | Source/Catalog | WB dilution |
|---|---|---|---|
| **Acetyl H3** | Rabbit | Millipore/06-599 | 1:1000 |
| **H3** | Rabbit | Cell Signaling/#9715 | 1:1000 |
| **Acetyl H4** | Sheep | R&D Systems/AF5215 | 1:1000 |
| **H4** | Rabbit | Cell Signaling/#2592 | 1:1000 |
| **HDAC2** | Rabbit | Abcam/ab-12169 | 1:1000 |
| **p-H2A.X S139** | Rabbit | Cell Signaling/#9718 | 1:1000 |
| **H2A.X** | Rabbit | Cell Signaling/#2595 | 1:1000 |
| **H3K9me2** | Rabbit | Cell Signaling/#4658 | 1:1000 |
| **TET2** | Mouse | Santa Cruz/sc-398535 | 1:500 |
| **β-Catenin** | Goat | Santa Cruz/sc-7963 | 1:500 |
| **BACE1** | Rabbit | Cell Signaling/#5606 | 1:2000 |
| **sAPPβ** | Rabbit | Covance/SIG-39139 | 1:1000 |
| **ADAM10** | Rabbit | Abcam/ab1997 | 1:1000 |
| **mTORC1** | Rabbit | Cell Signaling/#2501 | 1:1000 |
| **BCL2** | Mouse | Cell Signaling/#2870 | 1:1000 |
| **NRF2** | Rabbit | Santa Cruz/sc-722 | 1:500 |
| **GPX1** | Rabbit | Novus Biological/NBP1-33620 | 1:1500 |
| **SOD1** | Mouse | Calbiochem/574597 | 1:1000 |
| **Catalase** | Rabbit | Abcam/ab16731 | 1:1000 |
| **NF-κβ** | Rabbit | Cell Signaling/DE14E12 | 1:1000 |
| **p-Tau S396** | Rabbit | Invitrogen/44752G | 1:1000 |
| **p-Tau S404** | Rabbit | Invitrogen/44758G | 1:1000 |
| **Tau** | Goat | Santa Cruz/sc-1995 | 1:500 |
| **p-GSK3β S9** | Rabbit | Millipore/Clone 12B2 | 1:1000 |
| **GSK3β** | Rabbit | Cell Signaling/#9315 | 1:1000 |
| **Beclin 1** | Rabbit | Abcam/ab62557 | 1:1000 |
| **p-mTOR S2481** | Rabbit | Santa Cruz/sc-293089 | 1:500 |
| **mTOR** | Rabbit | Novus Biologicals/NB100-240 | 1:1000 |
| **LC3B** | Rabbit | Cell Signaling/#2775 | 1:1000 |
| **GAPDH** | Mouse | Millipore/MAB374 | 1:2000 |
| **β-Tubulin** | Mouse | Millipore/Clone AA2 | 1:2000 |
| **Goat-anti-mouse HRP conjugated** | | Biorad/170-5047 | 1:2000 |
| **Goat-anti-rabbit HRP conjugated** | | Biorad/170-6515 | 1:2000 |
| **Donkey-anti-goat HRP conjugated** | | Santa Cruz/sc-2020 | 1:2000 |

Preprints (www.preprints.org) | NOT PEER-REVIEWED | Posted: 21 January 2020 doi:10.20944/preprints202001.0244.v1

Peer-reviewed version available at Int. J. Mol. Sci. 2020, 21, 1154; doi:10.3390/ijms21031154

**Supplementary Table 2.** Primers and probes used in qPCR studies.

SYBR-Green primers

| Target | Product size (bp) | Forward primer (5'-3') | Reverse primer (5'-3') |
|---|---|---|---|
| ***Sirt1*** | 229 | AACACACACACAAAATCCAGCA | TGCAACCTGCTCCAAGGTAT |
| ***Sirt6*** | 147 | CGTTAATCGGTATGCCGT | GCAATTAGCGGATAACGG |
| ***Dnmt3a*** | 142 | TGCCAGACCTTGGAAACCTC | GCTGGCACCCTCTTCTTCAT |
| ***Aox1*** | 286 | CATAGGCGGCCAGGAACATT | TCCTCGTTCCAGAATGCAGC |
| ***Il-6*** | 112 | ATCCAGTTGCCTTCTTGGGACTGA | TAAGCCTCCGACTTGTGAAGTGGT |
| ***Il-10*** | 105 | GGCGCTGTCATCGATTTCT | TGGCCTTGTAGACACCTTG |
| ***Tnf-α*** | 157 | TCGGGGTGATCGGTCCCCAA | TGGTTTGCTACGACGTGGGCT |
| ***Gfap*** | 125 | CCTTCTGACACGGATTTGGT | ACATCGAGATCGCCACCTAC |
| ***Aβ-precursor*** | 99 | TCGGGGTGATCGGTCCCCAA | GTCACGTTCACCCTCCCCAG |
| ***β-actin*** | 218 | CTGTCCCTGTATGCCTCTG | ATGTCACGCACGATTTCC |

miRCURY LNA miRNA Validation probes

| Target | Reference |
|---|---|
| ***hsa-miR-29c-3p*** | YP00204729 |
| ***hsa-miR-431-5p*** | YP00204737 |
| ***mmu-miR-298-5p*** | YP00205092 |
| ***mmu-miR-98-5p*** | YP00204640 |
| ***hsa-miR-140-5p*** | YP00204540 |
| ***hsa-miR-181a-5p*** | YP00206081 |
| ***hsa-miR-106b-5p*** | YP00205884 |
| ***SNORD68*** | YP00203911 |

**Supplementary Table 3.** MicroRNAs differentially expressed in the hippocampus of SAMP8 compared to SAMR1. In bold significant changes in microRNAs gene expression. Chronic mild stress (CMS).

| miRNAs | t-test R1vsP8 (Control) | t-test R1vsP8 (CMS) | SAMP8 mean (Control) | SAMP8 mean (CMS) |
|---|---|---|---|---|
| **mmu-let-7c-5p** | 0,5206 | 0,8132 | 0,685515425 | 1,371331756 |
| **mmu-let-7e-5p** | **0,0811** | 0,5587 | 2,40490477 | 1,632769635 |
| **mmu-miR-106b-5p** | 0,9999 | 0,2660 | 1,132383859 | 1,232476548 |
| **mmu-miR-107-3p** | 0,8380 | 0,4660 | 1,328378691 | 3,799918898 |
| **mmu-miR-128-3p** | 0,4700 | 0,8359 | 1,019540454 | 0,770764343 |
| **mmu-miR-140-5p** | **0,0888** | 0,7931 | 0,427932135 | 0,638528798 |
| **mmu-miR-146a-5p** | 0,3321 | 0,9831 | 0,661767151 | 1,05660245 |
| **mmu-miR-148b-3p** | 0,5777 | 0,7738 | 0,850640236 | 1,358667617 |
| **mmu-miR-181a-5p** | 0,3322 | 0,5831 | 0,648670009 | 0,807795594 |
| **mmu-miR-191-5p** | 0,4023 | 0,7820 | 1,49960659 | 2,283907188 |
| **mmu-miR-26b-5p** | 0,9616 | 0,7750 | 1,256561233 | 2,40301896 |
| **mmu-miR-27a-3p** | 0,9834 | 0,4614 | 1,094208773 | 1,473142951 |
| **mmu-miR-29a-3p** | 0,6635 | 0,9001 | 0,781562275 | 0,780564672 |
| **mmu-miR-29c-3p** | 0,7673 | 0,2989 | 0,872848654 | 1,075036978 |
| **mmu-miR-431-5p** | 0,2351 | 0,3631 | 0,647237869 | 0,8543147 |
| **mmu-miR-484** | 0,4205 | 0,5736 | 0,697625273 | 0,85411048 |
| **mmu-miR-7a-5p** | 0,9262 | 0,1577 | 0,970688911 | 0,817409622 |
| **mmu-miR-9-5p** | 0,6745 | 0,7763 | 0,86533627 | 1,103131318 |
| **mmu-miR-98-5p** | 0,6566 | **0,0789** | 0,797413303 | 1,203181993 |
| **mmu-miR-101b-3p** | 0,7844 | 0,8586 | 0,973139682 | 1,197227365 |
| **mmu-miR-151-3p** | 0,3281 | **0,0705** | 0,670170619 | 1,655517937 |
| **mmu-miR-298-5p** | 0,5110 | 0,8686 | 0,506346238 | 1,199505517 |

**Supplementary Table 4.** MicroRNAs differentially expressed in the hippocampus of SAMP8 and SAMR1 under the influence of Chronic Mild Stress (CMS) compared to Control. In bold significant changes in microRNAs gene expression.

| miRNAs | t-test CMSvsCt (SAMR1) | t-test CMSvsCt (SAMP8) | CMS mean (SAMR1) | CMS mean (SAMP8) |
|---|---|---|---|---|
| **mmu-let-7c-5p** | 0,6702 | 0,4110 | 1,217779659 | 1,371331756 |
| **mmu-let-7e-5p** | 0,3220 | 0,2598 | 2,329973466 | 1,632769635 |
| **mmu-miR-106b-5p** | 0,4796 | 0,8131 | 0,674459492 | 1,232476548 |
| **mmu-miR-107-3p** | 0,1868 | 0,1199 | 2,889824565 | 3,799918898 |
| **mmu-miR-128-3p** | 0,2969 | 0,4166 | 0,721771206 | 0,770764343 |
| **mmu-miR-140-5p** | **0,0284** | 0,6703 | 0,520726166 | 0,638528798 |
| **mmu-miR-146a-5p** | 0,9188 | 0,5186 | 0,661767151 | 1,05660245 |
| **mmu-miR-148b-3p** | 0,9315 | 0,6381 | 1,007171102 | 1,358667617 |
| **mmu-miR-181a-5p** | 0,8769 | 0,6623 | 1,136036714 | 0,807795594 |
| **mmu-miR-191-5p** | 0,2235 | 0,5449 | 1,930735094 | 2,283907188 |
| **mmu-miR-26b-5p** | 0,4720 | 0,4802 | 1,945274377 | 2,40301896 |
| **mmu-miR-27a-3p** | 0,7589 | 0,4660 | 1,276677933 | 1,473142951 |
| **mmu-miR-29a-3p** | 0,5346 | 0,9984 | 0,731789022 | 0,780564672 |
| **mmu-miR-29c-3p** | 0,6103 | 0,6891 | 0,821643978 | 1,075036978 |
| **mmu-miR-431-5p** | 0,2273 | 0,3696 | 0,670621426 | 0,8543147 |
| **mmu-miR-484** | 0,4220 | 0,5712 | 0,705959538 | 0,85411048 |
| **mmu-miR-7a-5p** | 0,2673 | 0,1856 | 1,221853394 | 0,817409622 |
| **mmu-miR-9-5p** | 0,8555 | 0,4140 | 1,15465838 | 1,103131318 |
| **mmu-miR-98-5p** | 0,5442 | 0,3852 | 0,787400729 | 1,203181993 |
| **mmu-miR-101b-3p** | 0,8696 | 0,6396 | 1,281426619 | 1,197227365 |
| **mmu-miR-151-3p** | 0,6778 | 0,4055 | 1,172720512 | 1,655517937 |
| **mmu-miR-298-5p** | 0,9961 | 0,2580 | 1,085941122 | 1,199505517 |

Peer-reviewed version available at *Int. J. Mol. Sci.* **2020**, *21*, 1154; doi:10.3390/ijms21031154